

## Research Article

# Effect of Using Micropalm Oil Fuel Ash as Partial Replacement of Cement on the Properties of Cement Mortar

Kwangwoo Wi,<sup>1</sup> Han-Seung Lee,<sup>1</sup> Seungmin Lim ,<sup>1</sup> Mohamed A. Ismail,<sup>2</sup> and Mohd Warid Hussin<sup>3</sup>

<sup>1</sup>School of Architecture and Architectural Engineering, Hanyang University, Ansan, Gyeonggi-do, Republic of Korea

<sup>2</sup>Department of Civil Engineering, Miami College of Henan University, Kaifeng, Henan, China

<sup>3</sup>Construction Research Centre (UTM CRC), Institute for Smart Infrastructure and Innovative Construction, Universiti Teknologi Malaysia, 81310 UTM, Johor Bahru, Johor, Malaysia

Correspondence should be addressed to Seungmin Lim; [smlim09@hanyang.ac.kr](mailto:smlim09@hanyang.ac.kr)

Received 9 April 2018; Accepted 2 October 2018; Published 14 November 2018

Academic Editor: Wei Zhou

Copyright © 2018 Kwangwoo Wi et al. This is an open access article distributed under the Creative Commons Attribution License, which permits unrestricted use, distribution, and reproduction in any medium, provided the original work is properly cited.

This study investigates the effects of micropalm oil fuel ash (mPOFA) on compressive strength and pore structure of cement mortar. Various experimental techniques, such as compression test, isothermal calorimetry, mercury intrusion porosimetry, and X-ray diffraction, are performed to figure out the effect of using mPOFA as partial replacement of cement on the hydration of cement and determine its optimal replacement level to increase mechanical property of the mortar specimens. 10 wt.% of cement replacement with mPOFA is found to give the highest level of compressive strength, achieving a 23% increase over the control specimens after 3 days of curing. High  $K_2O$  contents in mPOFA stimulate  $C_3S$  in cement to form C-S-H at early ages, and high surface area of mPOFA acts as a nucleus to develop C-S-H. Also, small mPOFA particles and C-S-H formed by pozzolanic reaction fill the pores and lead to reduction in large capillary pores. In XRD analysis, a decrease in  $Ca(OH)_2$  and  $SiO_2$  contents with age confirmed a high pozzolanic reactivity of mPOFA.

## 1. Introduction

The production of cement consumes an enormous amount of raw materials and energy [1]. 3.2–6.3 GJ of energy and 1.7 tons of raw materials are consumed for every ton of clinker, resulting in the emission of approx. 850 kg of  $CO_2$  [2, 3]. As a result, cement production currently accounts for about 7% of global  $CO_2$  emissions [4], and this rate is expected to be increased, which demands to limit the production of cement clinker. This leads many scientific studies to be conducted for the development of alternative construction materials [5, 6] by utilizing industrial residues or agricultural residues [7]. Industrial residues, such as silica fume and fly ash, are widely used as supplementary cementitious materials (SCMs) due to their high pozzolanic reactivities [8–11]. There are also continuous efforts to develop agriculturally sourced pozzolanic materials, such

as rice husk ash (RHA) [12, 13], bamboo leaf ash (BLA) [14], corn cob ash (CCA) [15, 16] and palm oil fuel ash (POFA) [6,17–20].

As shown in Figure 1, POFA is generated by the combustion of agricultural residues, such as palm fibers and palm kernel shells in biomass thermal power plants [21]. Following the combustion, around 5% of the total solid is turned into POFA, which consists mainly of silica and alumina [22]. However, most of POFA is dumped as waste, which leads to soil contamination and other associated environmental problems [23]. Furthermore, the use of POFA is limited in cement and concrete industries because the surface area available for a reaction is too small when it is incorporated into cement-based composite materials. There are few studies [24, 25] that investigated how to increase the fineness of POFA, but the increased volume of plasticizer for the large amount of unburned carbon raises a problem [26].

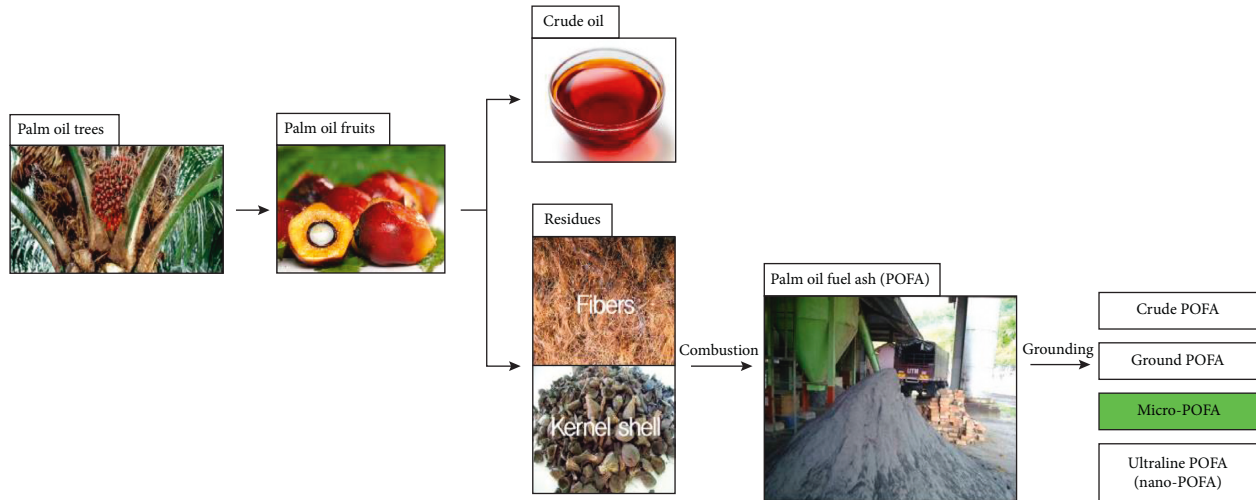


FIGURE 1: Production of palm oil fuel ash (POFA).

Further improvement of the fineness through an additional grinding process can solve the issue, after which the unburned carbon can be removed by drying the POFA in an oven at 500°C [25, 27].

Recent studies about POFA mostly focus on the effects of POFA on the durability and general properties of cement-based composite materials, such as the compressive strength of mortar and concrete [28, 29], the expansion rate [30], the heat of hydration [31–33], and the resistance to sulfate attack [34]. However, there is still lack of studies about the hydration properties and reactivity of very fine, micro-POFA (mPOFA) in a cement matrix. This study examines the hydration properties and reactivity of mPOFA in a cement matrix to determine the optimal replacement rate.

## 2. Experimental Program

### 2.1. Materials

**2.1.1. Cement.** Type I Ordinary Portland cement (OPC) was used in this study, which is defined by KS L 5201 [35]. Its physical properties and chemical composition are summarized in Table 1.

**2.1.2. Micropalm Oil Fuel Ash (mPOFA).** POFA was produced by the combustion of palm oil kernel shells and palm oil fibers at a palm oil mill, which is located in Johor, Malaysia. This POFA powder was dried in an oven at  $110 \pm 5^\circ\text{C}$  for 24h and then passed through a  $300\ \mu\text{m}$  sieve to remove coarse particles. The under-sized powder was further ground until 90% passed through a  $45\ \mu\text{m}$  sieve according to ASTM C618 [36]. This finely ground POFA is hereafter referred to as mPOFA. Its physical properties and chemical composition are shown in Table 1.

Figure 2 is an SEM image of mPOFA particles. It shows that mPOFA particles have sharp angles and irregular shapes as a result of being reduced in size by ball milling. There are also pores on the surface of mPOFA particles, which formed during the additional grinding [37].

TABLE 1: Physical properties and chemical composition of cement and mPOFA.

| Chemical composition                       | Cement (%) | mPOFA (%) |
|--|------------|-----------|
| SiO <sub>2</sub>                           | 19.47      | 70.9      |
| Al <sub>2</sub> O <sub>3</sub>             | 5.24       | 5.63      |
| Fe <sub>2</sub> O <sub>3</sub>             | 2.69       | 3.51      |
| CaO  | 61.8       | 3.78      |
| MgO  | 3.72       | 3.61      |
| SO <sub>3</sub>                            | 2.49       | —         |
| Na <sub>2</sub> O                          | 0.18       | 0.39      |
| K <sub>2</sub> O                           | 0.87       | 5.66      |
| LOI*                                       | 2.6        | 10.1      |
| <i>Physical properties</i>                 |            |           |
| Specific gravity (kg/m <sup>3</sup> )      | 3.15       | 2.3       |
| Specific surface area (cm <sup>2</sup> /g) | 3578       | 6091      |

\*LOI = loss on ignition.

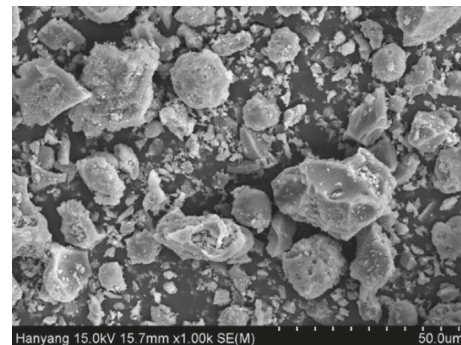


FIGURE 2: SEM image of mPOFA.

The XRD result of the mPOFA is presented in Figure 3. It confirms that mPOFA is a Si-rich material with main crystalline phases  $\alpha$ -quartz and cristobalite. This XRD pattern corresponds to the XRD results in the literature [1, 8, 26], which reported that POFA has about 70% amorphous content through semiquantitative and quantitative XRD analysis using the Rietveld method [27, 28].

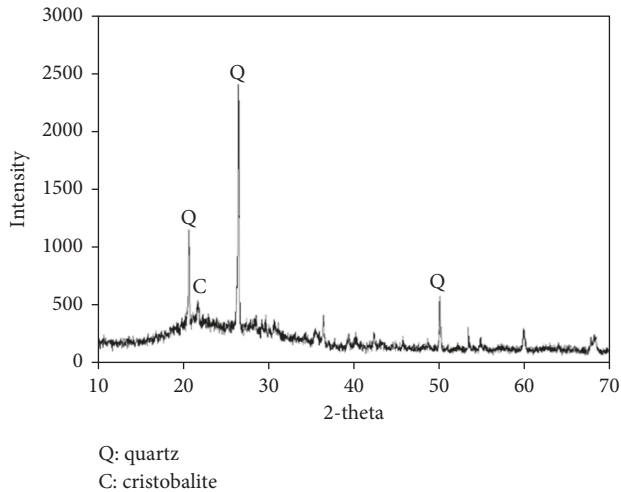


FIGURE 3: XRD pattern of mPOFA.

Thus, the mPOFA used in this study is expected to contain a similar amount of amorphous content.

**2.1.3. Fine Aggregates.** Siliceous sand was used as fine aggregates. Its physical properties are shown in Table 2.

**2.2. Mix Proportions.** Table 3 shows the mix proportion of mortar samples, which were prepared according to KS L ISO 679 [38]. Each sample was prepared by replacing 0, 10, 20, 30, or 40 wt.% of cement with mPOFA at a water-to-binder (cement + mPOFA) ratio of 50%. After casting, each mortar sample was cured at 20°C for 24 h prior to demolding. The samples were then cured in water at  $20 \pm 1^\circ\text{C}$  until reaching the age for each test. A separate set of samples without sand, cement paste, was prepared under the same conditions for X-ray diffraction (XRD) and scanning electron microscopy (SEM).

### 2.3. Test Methods

**2.3.1. Compressive Strength.** The compressive strength was measured on prismatic mortar specimens with 40 mm × 40 mm × 160 mm in accordance with KS L ISO 679 using the universal testing machine (UTM) after 3, 7, 14, and 28 days of curing. Testing was carried out on six specimens at each age, and the average value was reported.

**2.3.2. Heat of Hydration.** The heat of hydration was monitored for 72 h according to ASTM C1702 [39] (external mixing), using an isothermal conduction calorimeter (MMC-511SV, Tokyo Rico., LTD.). The samples were externally mixed before inserting them in the respective channels. It is noted that the data for the first 45 min were not considered for analysis to avoid the heat associated with mixing and lacing the externally prepared samples and to allow them to stabilize with the set temperature of 22°C.

**2.3.3. Pore Structure.** Small pieces (approx. 2 g in total) of mortar samples were soaked in acetone for 24 hours in a vacuum desiccator to stop hydration after 3 and 28 days of curing and then dried in an oven at 60°C for 24 h to remove any water. The pore structure of each sample was then examined using MIP (Autopore IV 9520) with maximum applied pressure of mercury, 400 MPa.

**2.3.4. Analysis of Hydration Products.** The crystal phases present in cement paste samples cured for 3 and 28 days were analyzed using XRD with a  $2\theta$  range between 10° and 70° at a scan rate of 5°/min.

## 3. Results and Discussion

**3.1. Compressive Strength of Cement Mortars Containing mPOFA.** Figure 4 shows the results of the compressive strength of mortar specimens at varying curing times and mPOFA contents. The specimens with an incorporation of 10% mPOFA by weight (POFA10) consistently produce the highest compressive strength, with a 33% increase over the control at 28 days of curing. The compressive strength of POFA20 was also consistently higher than the control specimen at all ages; however, there was a decrease in compressive strength if the replacement rate of mPOFA was increased any further.

The results show that the optimal replacement rate of mPOFA is 10% by weight, and the maximum replacement rate of mPOFA is 20% by weight. When mPOFA is replaced with cement at certain levels, the small mPOFA particles fill the pores between cement particles, thereby affecting the development of compressive strength [28, 34]. It is thought that the small particle size, silica content, and amorphous nature of mPOFA enabled it to act as nuclei in the cement matrix, which in turn stimulates the formation of C-S-H gel [19]. mPOFA is also a pozzolanic material, so  $\text{Ca}(\text{OH})_2$  that is formed by the cement hydration undergoes a pozzolanic reaction with the silica in mPOFA to produce secondary C-S-H [1, 27, 28]. However, the strength development worsened steadily at higher levels of mPOFA. By the replacement of cement with 40% of mPOFA, compressive strength at 28 days decreases by 77% in comparison with the control. Less cement content in specimens with higher levels of mPOFA could result in the reduction in compressive strength.

**3.2. Heat of Hydration.** Figure 5 shows the heat evolution rate of samples measured for 72 h after the initial mixing. When cement particles contact with water, it begins to generate heat (Stage 1); furthermore, it passes through a dormant period (Stage 2). After a few hours,  $\text{C}_3\text{S}$  begins to react actively and the heat evolution rate reaches a peak, referred to as second peak, at the end of the acceleration period (Stage 3) [40].

The heat evolution of POFA10 was the highest in Stage 3, with the peak starting earlier than with the control. This is thought to be caused by the alkali ions of mPOFA ( $\text{K}^+$  and  $\text{Na}^+$ ) promoting hydrolysis by stimulating  $\text{C}_3\text{S}$  and forming

TABLE 2: Physical properties of fine aggregates.

| Maximum size (mm) | Surface dry density (g/cm <sup>3</sup> ) | Absolute volume (%) | Fineness modulus (F.M) | Absorption rate (%) | Specific weight (kg/m <sup>3</sup> ) |
|-------------------|--|---------------------|------------------------|---------------------|--------------------------------------|
| 5.0               | 2.6                                      | 61.2                | 2.87                   | 1.02                | 1,590                                |

TABLE 3: Mix proportion of control mortar and mortar specimens containing mPOFA.

| Sample  | W/B (%) | Replacement ratio (%) | Cement (g) | POFA (g) | Sand (g) | Water (g) |
|---------|---------|-----------------------|------------|----------|----------|-----------|
| Control | 50      | 0                     | 450        | —        | 1350     | 225       |
| POFA10* | 50      | 10                    | 405        | 45       | 1350     | 225       |
| POFA20  | 50      | 20                    | 360        | 90       | 1350     | 225       |
| POFA30  | 50      | 30                    | 315        | 135      | 1350     | 225       |
| POFA40  | 50      | 40                    | 270        | 180      | 1350     | 225       |

\*POFA10 = replacement ratio of cement with mPOFA is 10%.

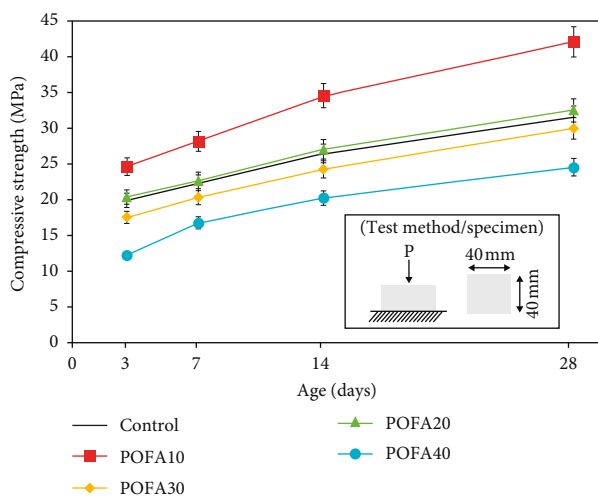


FIGURE 4: Compressive strength of mortars containing mPOFA.

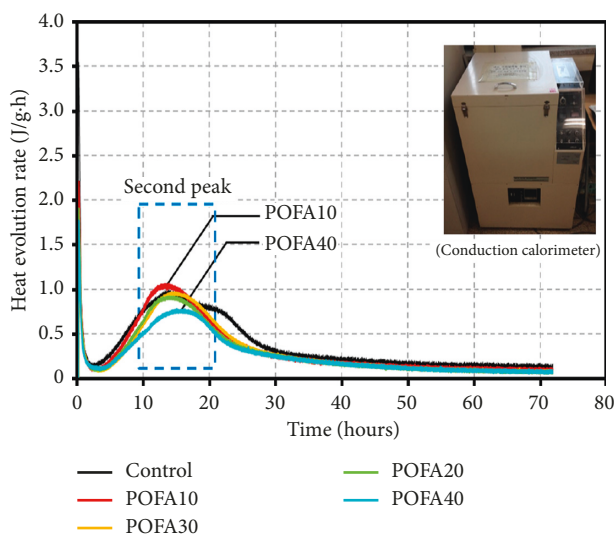


FIGURE 5: Heat evolution rate of mortars containing mPOFA.

C-S-H during the initial period [41, 42]. In addition, an increase in the mPOFA replacement rate decreased the size of the peak in Stage 3 and delayed the time of its occurrence [31].

Figure 6(a) shows the cumulative heat evolution over time, and Figure 6(b) shows the relative cumulative heat evolution according to the mPOFA contents, compared with the control. This reveals that the control had a higher cumulative heat (267 J/g) than POFA10 (233 J/g) and POFA40 (184 J/g), which confirmed that the cumulative heat decreases when the mPOFA content is increased. This result agrees well with that in previous research [33], which reported that 40% mPOFA replacement reduced the cumulative heat by 31% compared with the control. Again, high K<sub>2</sub>O content of mPOFA affects the hydration of cement through the stimulation of C<sub>3</sub>S. However, in view of the total amount of hydration heat, samples containing mPOFA showed lower cumulative heat evolution. This is because the total amount of cement for releasing heat lacked with the increasing replacement rate of mPOFA.

### 3.3. Pore Structure of Cement Mortar Containing mPOFA.

Figure 7 shows the pore size distribution of mortar samples, in which one can see that large capillary pores (0.05–10 μm in size) in POFA10 and POFA20 are either less or equal in quantity to those in the control after 3 days of curing. In contrast, POFA30 and POFA40 had either more or an equal number of large capillary pores as the control. Consequently, it is thought that the mPOFA particles effectively fill the pores in mortar specimens with 10–20% mPOFA replacement [28], which is consistent with their greater compressive strength.

After curing for 28 days, the amounts of pores larger than 0.1 μm in diameter decreased in all samples compared with 3 days of curing, but the pores smaller than 0.1 μm increased in all samples except the control. This is attributed to the formation of hydration products in the large capillary pores, which increases the number of midsized (0.01–0.5 μm diameter) capillary pores. The cumulative pore volume of the mortar samples containing mPOFA is shown in Figure 8. The volume of pores 0.1 μm in diameter or larger increased with mPOFA replacement at 3 days of curing. In addition, the gel pores of 0.01 μm in diameter or less were only observed in mortars with 10 or 20% mPOFA replacement. With 28 days of curing, the cumulative pore volume of most of the samples decreased, and the volume of pores greater

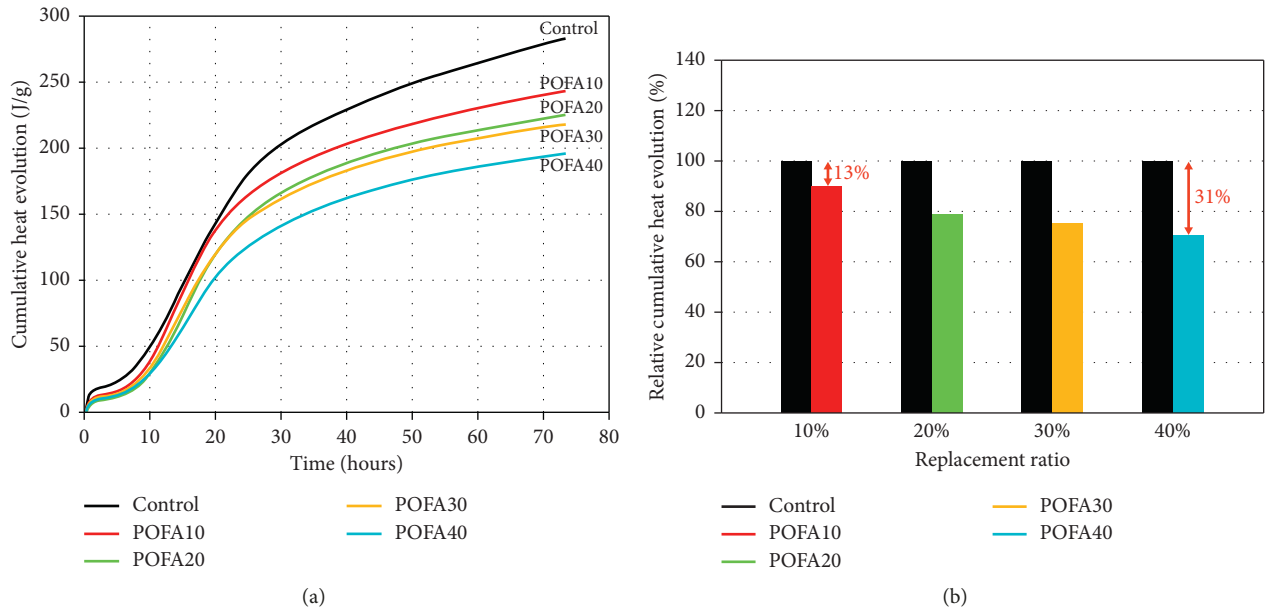


FIGURE 6: (a) Cumulative heat evolution of mortars containing mPOFA. (b) Relative cumulative heat evolution of mortars containing mPOFA.

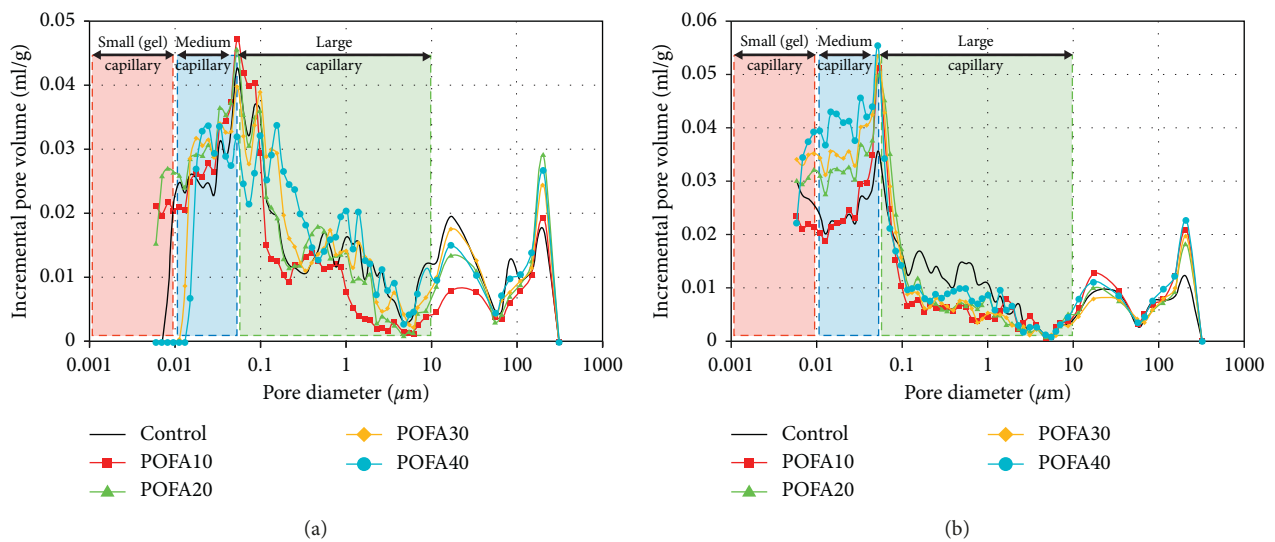


FIGURE 7: Pore distribution of mortars containing mPOFA aged for (a) 3 and (b) 28 days.

than  $0.1 \mu\text{m}$  in diameter was greater in the control than that in the samples with mPOFA.

The pore size distribution of concrete is closely related to its permeability which governs durability. The pores can be categorized as gel, medium, large capillary pores, or air voids depending on their size [40]. The gel pores, which constitute the internal porosity of C-S-H, were observed in POFA10 and POFA20 after 3 days of curing. It is thought that mPOFA affects the development of C-S-H at early ages.

**3.4. Phase Analysis of Cement Paste Containing mPOFA.** The XRD results are shown in Figure 9.  $\text{Ca}(\text{OH})_2$  and  $\text{SiO}_2$  peaks were observed in all samples at 3 days of curing. As the

replacement level of mPOFA increased, the  $\text{Ca}(\text{OH})_2$  peak decreased and the  $\text{SiO}_2$  peak increased owing to the replacement of cement with mPOFA; that is, the volume of  $\text{Ca}^{2+}$  needed to produce  $\text{Ca}(\text{OH})_2$  decreased because mPOFA is predominantly silica. After 28 days of curing,  $\text{Ca}(\text{OH})_2$  and  $\text{SiO}_2$  peaks were again observed in all samples; however, the peak of  $\text{Ca}(\text{OH})_2$  decreased compared with 3 days. This is because  $\text{Ca}(\text{OH})_2$  and  $\text{SiO}_2$  were consumed to produce C-S-H by pozzolanic reaction.

**3.5. Role of mPOFA in Cement Hydration.** A schematic diagram of the role of mPOFA in a cement hydration is provided in Figure 10, which is drawn based on the

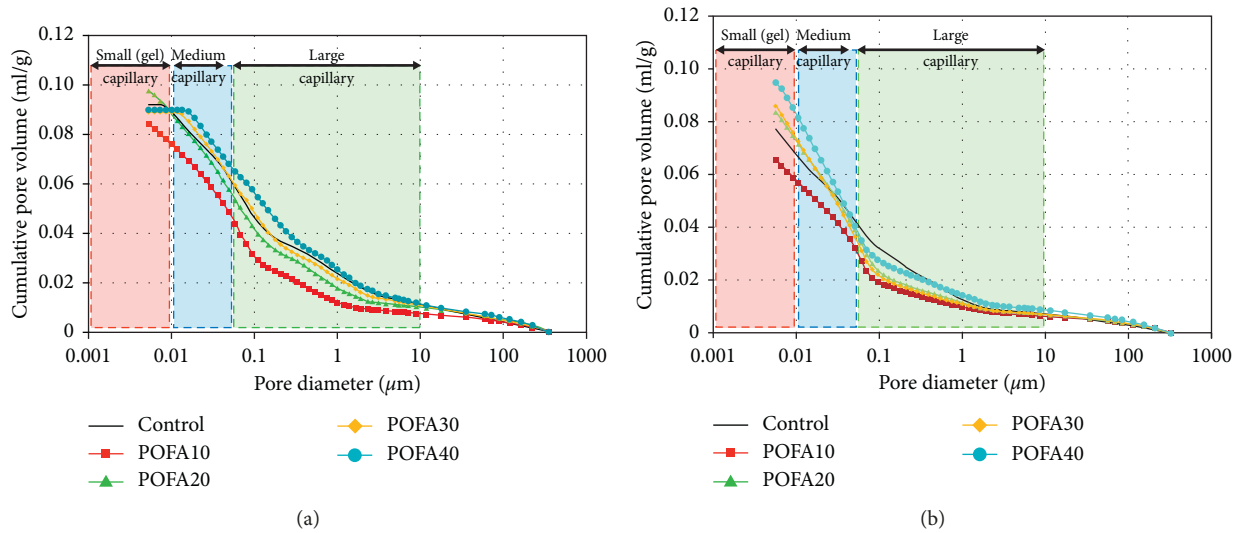


FIGURE 8: Cumulative pore volume of mortars containing mPOFA aged for (a) 3 and (b) 28 days.

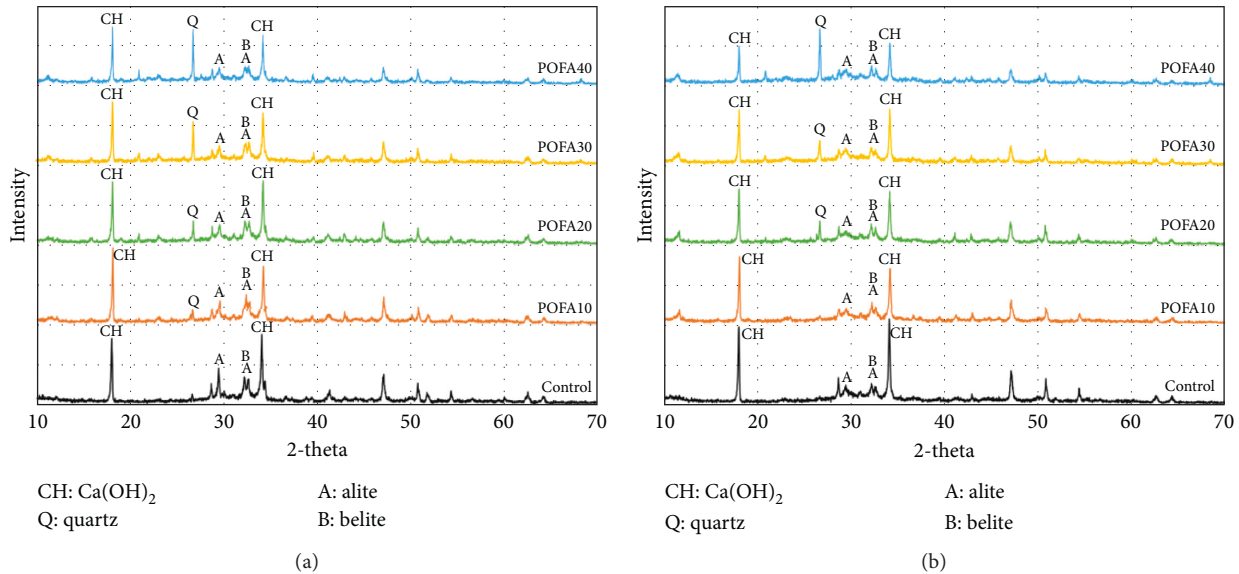


FIGURE 9: XRD patterns of pastes containing mPOFA aged for (a) 3 and (b) 28 days.

experimental results. When mPOFA particles contact with water, alkali ions ( $K^+$ ,  $Na^+$ ), which weakly bound to mPOFA, are easily eluted, thereby making the mPOFA surface negatively charged with electrons. The eluted alkali ions subsequently stimulate the hydrolysis of  $C_3S$  in cement clinker, which increases the concentration of  $Ca^{2+}$  ions in solution [43] as confirmed by isothermal calorimetry.

As the elution of alkali ions is the ongoing process, the concentration of alkali ions in solution steadily increases and a Si-rich zone is formed around the surface of the mPOFA particle. Over time,  $SiO_4^{4-}$  ions in the Si-rich zone are eluted by osmotic pressure and then react with  $Ca^{2+}$  to form C-S-H. It is thought that mPOFA particles play a role in this process by providing a nucleus for C-S-H growth due to their high specific surface area [44]. After further curing,  $Ca(OH)_2$  and

$SiO_2$  were consumed to produce C-S-H through pozzolanic reaction, which probably blocks the pores and thus makes a dense microstructure.

#### 4. Conclusions

This study examines the effects of an agricultural waste, mPOFA, on changes in compressive strength and pore structure of cement mortar. An optimal replacement rate, 10 wt.% of cement with mPOFA is determined for maximizing its utility as a supplementary cementitious material. Based on various experimental results, the following conclusions are drawn.

A 10 wt.% replacement of cement with mPOFA yields the highest compressive strength at all ages, with a 33% increase in strength over the control at 28 days. This could be

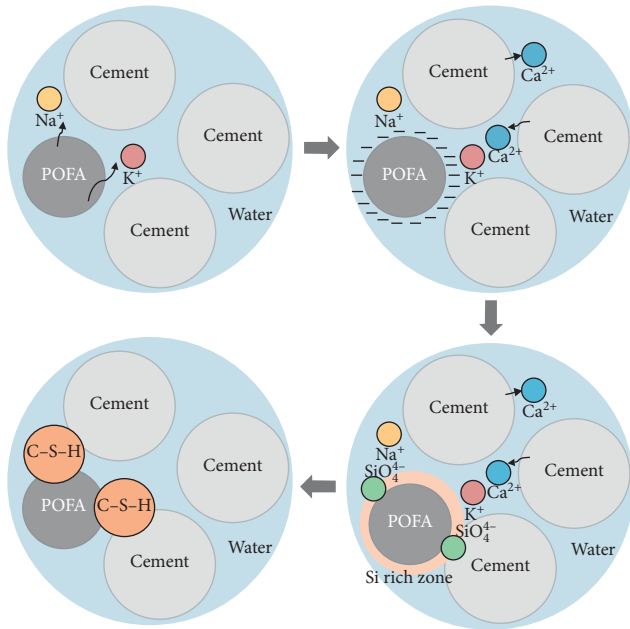


FIGURE 10: Role of mPOFA in cement hydration.

due to mPOFA filling the space between cement particles and promoting the formation of C-S-H.

Increasing the amount of mPOFA reduces the compressive strength, but the difference in strength between POFA40 and the control decreased by 27% with a prolonged curing of 28 days. This is attributed to the Si-rich mPOFA particles reacting with  $\text{Ca}(\text{OH})_2$  formed during cement hydration to produce secondary C-S-H.

The rate of heat evolution generally decreased with increasing mPOFA content, but POFA10 exhibited a higher rate and earlier peak than the control in Stage 2. This could be the result of alkali ions eluted from mPOFA stimulating the hydrolysis of  $\text{C}_3\text{S}$ .

The incorporation of 10% and 20% mPOFA produced fewer large capillary pores, which is most likely the result of filling the spaces between cement particles by mPOFA particles and newly formed C-S-H.

High levels of  $\text{K}_2\text{O}$  in mPOFA stimulate the hydrolysis of  $\text{C}_3\text{S}$  in cement, and mPOFA particles with high surface area acts as nuclei for hydration. Consequently, pores are probably filled with C-S-H formed by pozzolanic reaction, which makes a dense microstructure and refines the pore structure.

## Data Availability

The data used to support the findings of this study are included within the article.

## Conflicts of Interest

The authors declare no conflict of interest.

## Acknowledgments

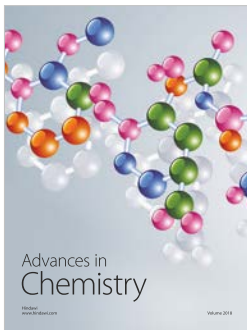
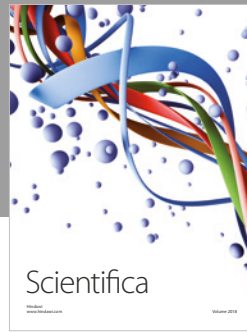
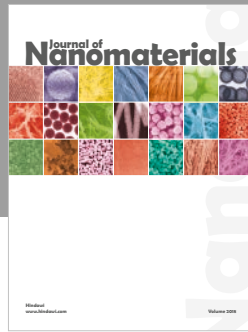
This research was supported by basic science research program through the National Research Foundation (NRF)

of Korea funded by the Ministry of Science, ICT and Future Planning (No. 2015R1A5A1037548).

## References

- [1] T. Sinsiri, W. Kroehong, C. Jaturapitakkul, and P. Chindapasirt, "Assessing the effect of biomass ashes with different finenesses on the compressive strength of blended cement paste," *Materials and Design*, vol. 42, pp. 424–433, 2012.
- [2] H. G. Oss and A. C. Padovani, "Cement manufacture and the environment: part I: chemistry and technology," *Journal of Industrial Ecology*, vol. 6, no. 1, pp. 89–105, 2002.
- [3] H. G. Oss and A. C. Padovani, "Cement manufacture and the environment part II: environmental challenges and opportunities," *Journal of Industrial Ecology*, vol. 7, no. 1, pp. 93–126, 2003.
- [4] V. M. Malhotra, "Global warming, and role of supplementary cementing materials and superplasticisers in reducing greenhouse gas emissions from the manufacturing of portland cement," *International Journal of Structural Engineering*, vol. 1, no. 2, pp. 116–130, 2010.
- [5] V. Sata, C. Jaturapitakkul, and K. Kiattikomol, "Influence of pozzolan from various by-product materials on mechanical properties of high-strength concrete," *Construction and Building Materials*, vol. 21, no. 7, pp. 1589–1598, 2007.
- [6] E. Aprianti, P. Shafiqh, S. Bahri, and J. N. Farahani, "Supplementary cementitious materials origin from agricultural wastes—A review," *Construction and Building Materials*, vol. 74, pp. 176–187, 2015.
- [7] E. Aprianti, "A huge number of artificial waste material can be supplementary cementitious material (SCM) for concrete production—a review part II," *Journal of Cleaner Production*, vol. 142, pp. 4178–4194, 2017.
- [8] S. Chatterji, N. Thaulow, and P. Christensen, "Puzzolanic activity of byproduct silica-fume from ferro-silicom production," *Cement and Concrete Research*, vol. 12, no. 6, pp. 781–784, 1982.
- [9] P. K. Mehta and O. E. Gjörv, "Properties of portland cement concrete containing fly ash and condensed silica-fume," *Cement and Concrete Research*, vol. 12, no. 5, pp. 587–595, 1982.
- [10] S. Diamond, "The utilization of flyash," *Cement and Concrete Research*, vol. 14, no. 4, pp. 455–462, 1984.
- [11] P. Chindapasirt, C. Jaturapitakkul, and T. Sinsiri, "Effect of fly ash fineness on microstructure of blended cement paste," *Construction and Building Materials*, vol. 21, no. 7, pp. 1534–1541, 2007.
- [12] G. R. De Sensale, "Effect of rice-husk ash on durability of cementitious materials," *Cement and Concrete Composites*, vol. 32, no. 9, pp. 718–725, 2010.
- [13] M. F. M. Zain, M. N. Islam, F. Mahmud, and M. Jamil, "Production of rice husk ash for use in concrete as a supplementary cementitious material," *Construction and Building Materials*, vol. 25, no. 2, pp. 798–805, 2011.
- [14] E. Villar-Cociña, E. V. Morales, S. F. Santos, H. Savastano, and M. Frías, "Pozzolanic behavior of bamboo leaf ash: characterization and determination of the kinetic parameters," *Cement and Concrete Composites*, vol. 33, no. 1, pp. 68–73, 2011.
- [15] D. A. Adesanya and A. A. Raheem, "Development of corn cob ash blended cement," *Construction and Building Materials*, vol. 23, no. 1, pp. 347–352, 2009.
- [16] D. A. Adesanya and A. A. Raheem, "A study of the permeability and acid attack of corn cob ash blended cements," *Construction and Building Materials*, vol. 24, no. 3, pp. 403–409, 2010.

- [17] W. Kroehong, T. Sinsiri, and C. Jaturapitakkul, "Effect of palm oil fuel ash fineness on packing effect and pozzolanic reaction of blended cement paste," *Procedia Engineering*, vol. 14, pp. 361–369, 2011.
- [18] N. H. A. S. Lim, M. A. Ismail, H. S. Lee, M. W. Hussin, A. R. M. Sam, and M. Samadi, "The effects of high volume nano palm oil fuel ash on microstructure properties and hydration temperature of mortar," *Construction and Building Materials*, vol. 93, pp. 29–34, 2015.
- [19] M. A. A. Rajak, Z. A. Majid, and M. Ismail, "Morphological characteristics of hardened cement pastes incorporating nano-palm oil fuel ash," *Procedia Manufacturing*, vol. 2, pp. 512–518, 2015.
- [20] M. M. U. Islam, K. H. Mo, U. J. Alengaram, and M. Z. Jumaat, "Mechanical and fresh properties of sustainable oil palm shell lightweight concrete incorporating palm oil fuel ash," *Journal of Cleaner Production*, vol. 115, pp. 307–314, 2016.
- [21] W. Tangchirapat, C. Jaturapitakkul, and P. Chindaprasirt, "Use of palm oil fuel ash as a supplementary cementitious material for producing high-strength concrete," *Construction and Building Materials*, vol. 23, no. 7, pp. 2641–2646, 2009.
- [22] J. H. Tay and K. Y. Show, "Use of ash derived from oil-palm waste incineration as a cement replacement material," *Resources, Conservation and Recycling*, vol. 13, no. 1, pp. 27–36, 1995.
- [23] A. S. M. A. Awal and S. K. Nguong, "A short-term investigation on high volume palm oil fuel ash (POFA) concrete," in *Proceedings of 35th Conference on Our World in Concrete and Structure*, pp. 85–92, Singapore, August 2010.
- [24] J. H. Tay, "Ash from oil-palm waste as a concrete material," *Journal of Materials in Civil Engineering*, vol. 2, no. 2, pp. 94–105, 1990.
- [25] W. Tangchirapat, T. Saeting, C. Jaturapitakkul, K. Kiattikomol, and A. Siripanichgorn, "Use of waste ash from palm oil industry in concrete," *Waste Management*, vol. 27, no. 1, pp. 81–88, 2007.
- [26] C. Chandara, E. Sakai, K. A. M. Azizli, Z. A. Ahmad, and S. F. S. Hashim, "The effect of unburned carbon in palm oil fuel ash on fluidity of cement pastes containing superplasticizer," *Construction and Building Materials*, vol. 24, no. 9, pp. 1590–1593, 2010.
- [27] W. Kroehong, T. Sinsiri, C. Jaturapitakkul, and P. Chindaprasirt, "Effect of palm oil fuel ash fineness on the microstructure of blended cement paste," *Construction and Building Materials*, vol. 25, no. 11, pp. 4095–4104, 2011.
- [28] C. Jaturapitakkul, J. Tangpagasit, S. Songmue, and K. Kiattikomol, "Filler effect and pozzolanic reaction of ground palm oil fuel ash," *Construction and Building Materials*, vol. 25, no. 11, pp. 4287–4293, 2011.
- [29] W. Tangchirapat and C. Jaturapitakkul, "Strength, drying shrinkage, and water permeability of concrete incorporating ground palm oil fuel ash," *Cement and Concrete Composites*, vol. 32, no. 10, pp. 767–774, 2010.
- [30] A. A. Awal and M. W. Hussin, "The effectiveness of palm oil fuel ash in preventing expansion due to alkali-silica reaction," *Cement and Concrete Composites*, vol. 19, no. 4, pp. 367–372, 1997.
- [31] A. A. Awal and M. W. Hussin, "Effect of palm oil fuel ash in controlling heat of hydration of concrete," *Procedia Eng*, vol. 14, pp. 2650–2657, 2011.
- [32] C. Chandara, K. A. M. Azizli, Z. A. Ahmad, S. F. S. Hashim, and E. Sakai, "Heat of hydration of blended cement containing treated ground palm oil fuel ash," *Construction and Building Materials*, vol. 27, no. 1, pp. 78–81, 2012.
- [33] A. A. Awal and I. A. Shehu, "Evaluation of heat of hydration of concrete containing high volume palm oil fuel ash," *Fuel*, vol. 105, pp. 728–731, 2013.
- [34] C. Jaturapitakkul, K. Kiattikomol, W. Tangchirapat, and T. Saeting, "Evaluation of the sulfate resistance of concrete containing palm oil fuel ash," *Construction and Building Materials*, vol. 21, no. 7, pp. 1399–1405, 2007.
- [35] KS L 5201, *Portland Cement*, Korean Standards Association, Seoul, Republic of Korea, 2013.
- [36] ASTM C 618, *Standard Specification for Coal Fly Ash and Raw or Calcined Natural Pozzolan for Use in Concrete*, ASTM International, West Conshohocken, PA, USA, 2012.
- [37] M. R. Karim, M. F. M. Zain, M. Jamil, and F. C. Lai, "Fabrication of a non-cement binder using slag, palm oil fuel ash and rice husk ash with sodium hydroxide," *Construction and Building Materials*, vol. 49, pp. 894–902, 2013.
- [38] KS L ISO 679, *Methods of Testing Cements-Determination of Strength*, Korean Standards Association, Seoul, 2010.
- [39] ASTM C1702, *Standard Test Method for Measurement of Heat of Hydration of Hydraulic Cementitious Materials Using Isothermal Conduction Calorimetry*, ASTM International, West Conshohocken, PA, USA, 2009.
- [40] S. Mindess, J. F. Young, and D. Darwin, *Concrete*, Prentice-Hall, Upper Saddle River, NJ, USA, 2nd edition, 2003.
- [41] I. Jawed and J. Skalny, "Alkalies in cement: a review: II. Effects of alkalies on hydration and performance of Portland cement," *Cement and Concrete Research*, vol. 8, no. 1, pp. 37–51, 1978.
- [42] O. Mendoza, C. Giraldo, S. S. Camargo, and J. I. Tobón, "Structural and nano-mechanical properties of Calcium Silicate Hydrate (CSH) formed from alite hydration in the presence of sodium and potassium hydroxide," *Cement and Concrete Research*, vol. 74, pp. 88–94, 2015.
- [43] S. H. Lee, "Pozzolan reaction," *Cement*, vol. 158, p. 40, 2003.
- [44] L. P. Singh, S. R. Karade, S. K. Bhattacharyya, M. M. Yousuf, and S. Ahalawat, "Beneficial role of nanosilica in cement based materials—A review," *Construction and Building Materials*, vol. 47, pp. 1069–1077, 2013.



**Hindawi**  
Submit your manuscripts at  
[www.hindawi.com](http://www.hindawi.com)

